

Simultaneous Measurement of ^1H – ^{15}N , ^1H – $^{13}\text{C}'$, and ^{15}N – $^{13}\text{C}'$ Dipolar Couplings in a Perdeuterated 30 kDa Protein Dissolved in a Dilute Liquid Crystalline Phase

Yun-Xing Wang,[†] John L. Marquardt,[‡] Paul Wingfield,[§]
Stephen J. Stahl,[§] Sylvia Lee-Huang,^{||} Dennis Torchia,[†] and
Ad Bax^{*,§}

Molecular Structural Biology Unit, National
Institute of Dental Research, Protein Expression
Laboratory, National Institute of Arthritis and
Musculoskeletal and Skin Diseases, and Laboratory
of Chemical Physics, National Institute of Diabetes
and Digestive and Kidney Diseases, National
Institutes of Health, Bethesda, Maryland 20892
Department of Biochemistry, New York University
School of Medicine, New York, New York 10016

Received March 16, 1998

Residual one-bond dipolar couplings in high-resolution NMR provide unique constraints in molecular structure determination.^{1–3} As the internuclear distance for such dipolar interactions is essentially fixed, the dipolar couplings yield direct information on the orientations of the corresponding bond vectors relative to the molecular alignment tensor. These constraints are therefore very different from NOE and J couplings, which constrain atom positions only relative to their immediately adjacent neighbors. Addition of a small number of ^1H – ^{15}N and ^1H – $^{13}\text{C}'$ one-bond dipolar constraints, measured for a protein complexed with a 16-base pair DNA fragment, resulted in a nearly 2-fold reduction of ϕ/ψ pairs outside the most-favored region of the Ramachandran map⁴ and greatly improved the agreement between predicted and measured magnetic field dependence of ^{15}N shift.⁵

Use of a liquid crystalline phase of planar phospholipid micelles, commonly referred to as bicelles,⁶ appears to offer a generally applicable method to cause a weak degree of protein alignment.⁷ Here, we demonstrate that in perdeuterated proteins at high magnetic field strengths the ^{15}N line-narrowing, obtained by constructive use of relaxation interference^{8,9} between ^{15}N – ^1H dipolar coupling and ^{15}N chemical shift anisotropy (CSA), permits accurate measurement of even the small couplings between $^{13}\text{C}'$ and ^{15}N . In addition, accurate values of the two-bond dipolar coupling between $^{13}\text{C}'$ and ^1H and the one-bond ^1H – ^{15}N coupling can be derived from the same data set.

Pervushin et al.⁹ predict that relaxation interference results in the narrowest ^{15}N line widths at magnetic field strengths corre-

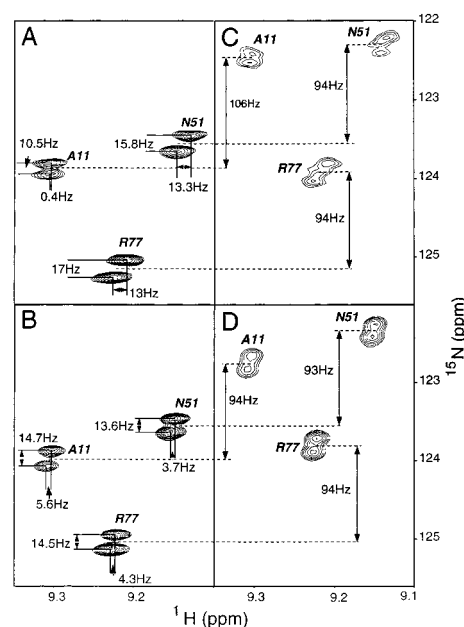


Figure 1. Small sections of the IPAP-[^1H – ^{15}N]-HSQC spectrum of U-(^{15}N , ^{13}C , ^2H) MAP30, recorded at 750 MHz ^1H frequency, in the absence of ^{13}C decoupling. (A and B) Downfield ^{15}N – ^1H multiplet components and (C and D) upfield multiplet components; (A and C) 0.15 mM MAP30 in the liquid crystalline phase and (B and D) 0.7 mM MAP30 in the isotropic phase. The measurement in the isotropic phase took 6 h; the measurement in the liquid crystalline phase took 20 h.

sponding to slightly over 1 GHz ^1H frequency and that high ^{15}N resolution is obtainable even for large, slowly tumbling perdeuterated molecules. Although NOEs between backbone amide protons in perdeuterated proteins are readily measured,¹⁰ they are generally insufficiently constraining to obtain more than an approximate fold of the polypeptide.¹¹ However, with the additional availability of accurate dipolar constraints for the polypeptide backbone, the requirement to obtain a very large number of NOEs is considerably reduced. Therefore, accurate measurement of small heteronuclear dipolar couplings, shown here to be possible by constructive use of relaxation interference, opens the opportunity to extend the size limit of protein structure determination by NMR considerably.

Figure 1 compares a small region of the 750 MHz ^{15}N – ^1H HSQC spectrum of the 30 kDa ribosomal inactivating protein MAP30 recorded in the liquid crystalline phase [0.15 mM U- $\{^2\text{H}, ^{13}\text{C}, ^{15}\text{N}\}$ MAP30; 67 mM DMPC, 22.5 mM DHPC (5wt %/v total phospholipid) in 220 μL 95% H_2O , 5% D_2O ; 10 mM sodium phosphate, pH 5.5; 36 $^\circ\text{C}$] (Figure 1, A and C), with that recorded for a 0.7 mM sample in the isotropic state (Figure 1, B and D). The spectra shown correspond to the sum and difference of two data sets; one recorded with the two ^{15}N – $\{^1\text{H}\}$ F_1 doublet components in-phase (IP) relative to one another; the other with anti-phase (AP) F_1 doublets,^{9,12,13} and the pulse scheme used (Describing Information) is very similar to the previously described IPAP–HSQC pulse scheme¹³ but lacks ^{13}C decoupling in the F_1 dimension. As a result of relaxation interference between the ^{15}N CSA and the ^{15}N – ^1H dipolar coupling, the spectra

[†] National Institute of Dental Research.

[‡] National Institute of Arthritis and Musculoskeletal and Skin Diseases.

[§] National Institute of Diabetes and Digestive and Kidney Diseases.

^{||} New York University School of Medicine.

(1) Sauepe, A.; Englert, G. *Phys. Rev. Lett.* **1963**, *11*, 462–465. Emsley, J. W.; Linton, J. C. *NMR Spectroscopy using liquid crystal solvents*; Pergamon Press: New York, 1975. Drobny, G. in *Nuclear Magnetic Resonance of Liquid Crystals*; Emsley, J. W., Ed.; Reidel: Boston, MA, 1983; pp 289–314.

(2) Bastiaan, E. W.; MacLean, C.; van Zijl, P. C. M.; Bothner-By, A. A. *Annu. Rep. NMR Spectrosc.* **1987**, *9*, 35–77. Bothner-By, A. A. *Encyclopedia of Nuclear Magnetic Resonance*; Grant, D. M., Harris, R. K., Eds; Wiley: Chichester, 1996; pp 2932–2938.

(3) Tolman, J. R.; Flanagan, J. M.; Kennedy, M. A.; Prestegard, J. H. *Proc. Natl. Acad. Sci. U.S.A.* **1995**, *92*, 9279–9283. King, H. C.; Wang, K. Y.; Goljer, I.; Bolton, P. H. *J. Magn. Reson. Ser. B* **1995**, *109*, 323–325. Tjandra, N.; Grzesiek, S.; Bax, A. *J. Am. Chem. Soc.* **1996**, *118*, 6264–6272.

(4) Tjandra, N.; Omichinski, J. G.; Gronenborn, A. M.; Clore, G. M.; Bax, A. *Nat. Struct. Biol.* **1997**, *4*, 732–738.

(5) Ottiger, M.; Tjandra, N.; Bax, A. *J. Am. Chem. Soc.* **1997**, *119*, 9825–9830.

(6) Sanders, C. R.; Schwonek, J. P. *Biochemistry* **1992**, *31*, 8898–8905.

(7) Bax, A.; Tjandra, N. *J. Biomol. NMR* **1997**, *10*, 289–292. Tjandra, N.; Bax, A. *Science* **1997**, *278*, 1111–1114.

(8) Goldman, M. *J. Magn. Reson.* **1984**, *60*, 437–452. Tjandra, N.; Szabo, A.; Bax, A. *J. Am. Chem. Soc.* **1996**, *118*, 6986–6991.

(9) Pervushin, K.; Wider, G.; Wüthrich, K. *Proc. Natl. Acad. Sci. U.S.A.* **1997**, *94*, 12366–12371.

(10) Venters, R. A.; Metzler, W. J.; Spicer, L. D.; Mueller, L.; Farmer, B. T. *J. Am. Chem. Soc.* **1995**, *117*, 9594–9595. Grzesiek, S.; Wingfield, P.; Stahl, S.; Kaufman, J.; Bax, A. *J. Am. Chem. Soc.* **1995**, *117*, 9596–9597.

(11) Kay, L. E.; Gardner, K. H. *Curr. Opin. Struct. Biol.* **1997**, *7*, 722–731.

(12) Meissner, A.; Duus, J. Ø.; Sørensen, O. W. *J. Biomol. NMR* **1997**, *10*, 89–94.

(13) Ottiger, M.; Bax, A. *J. Magn. Reson.* **1998**, *131*, 373–378.

containing the downfield ^{15}N doublet components (Figure 1, A and B) display much higher resolution than the spectra containing the upfield components (Figure 1, C and D). Relative vertical displacement of the multiplet components within each panel is due to ^{13}C – ^{15}N coupling and corresponds to the sum of $^1J_{\text{C}'\text{N}} + ^1D_{\text{C}'\text{N}}$ (Figure 1A), whereas in the isotropic state this splitting is $^1J_{\text{C}'\text{N}}$ (Figure 1B). Similarly, relative horizontal displacement of the two doublet components in Figure 1A corresponds to $^2J_{\text{C}'\text{H}^{\text{N}}} + ^2D_{\text{C}'\text{H}^{\text{N}}}$; the analogous displacement in the isotropic state equals $^2J_{\text{C}'\text{H}^{\text{N}}}$. The $^1J_{\text{H}^{\text{N}}} + ^1D_{\text{H}^{\text{N}}}$ splitting is obtained from the difference in peak position in the F_1 (^{15}N) dimension between Figure 1, A and C, whereas $^1J_{\text{H}^{\text{N}}}$ is measured from Figure 1 B and D.

The resolution in the horizontal ($^1\text{H}^{\text{N}}$) dimension benefits from the perdeuteration of the protein, enhancing the accuracy with which $^2D_{\text{C}'\text{H}^{\text{N}}}$ can be measured. Although not used in the present study, even higher resolution in this dimension can be obtained by selecting only the upfield $^1\text{H}^{\text{N}}$ – $\{^{15}\text{N}\}$ doublet component and thereby utilizing the effect of relaxation interference between the $^1\text{H}^{\text{N}}$ CSA and the ^1H – ^{15}N dipolar coupling.⁹

The dipolar coupling between two nuclei, A and B, in a solute macromolecule of fixed shape is given by

$$D^{\text{AB}}(\alpha, \beta) = D_a^{\text{AB}} \{ (3 \cos^2 \alpha - 1) + \frac{3}{2} R (\sin^2 \alpha \cos 2\beta) \} \quad (1)$$

where R is the rhombicity defined by $D_r^{\text{AB}}/D_a^{\text{AB}}$ and is always positive; D_a^{AB} and D_r^{AB} (in units of hertz) are the axial and rhombic components of the traceless second rank diagonal tensor \mathbf{D} given by $\frac{1}{3}[D_{zz}^{\text{AB}} - (D_{xx}^{\text{AB}} + D_{yy}^{\text{AB}})/2]$ and $\frac{1}{3}[D_{xx}^{\text{AB}} - D_{yy}^{\text{AB}}]$, respectively, with $|D_{zz}^{\text{AB}}| > |D_{yy}^{\text{AB}}| \geq |D_{xx}^{\text{AB}}|$; α and β are the spherical polar angles defining the A–B interatomic vector in the principal axis frame of the alignment tensor. D_a^{AB} subsumes various constants, including the gyromagnetic ratios of the two nuclei γ_A and γ_B , the inverse cube of the distance between the two nuclei, $\langle r_{\text{AB}}^{-3} \rangle$, where the broken brackets indicate vibrational averaging, and the generalized order parameter S for fast angular fluctuations of the internuclear vector¹⁴ which provides a first-order correction for the effect of rapid internal motion on D^{AB} . In the liquid crystal bicelle medium

$$D_a^{\text{AB}} = -(\mu_0 h / 16\pi^3) S \gamma_A \gamma_B \langle r_{\text{AB}}^{-3} \rangle A_a \quad (2)$$

where A_a is the unitless axial component of the molecular alignment tensor \mathbf{A} .

As described elsewhere,¹⁵ accurate estimates for the magnitude and rhombicity of \mathbf{A} in the absence of knowledge of the protein's structure can be obtained from the ranges of values observed for the various types of dipolar couplings. The orientation of a peptide group relative to this alignment tensor is described by three Euler angles, which can be calculated from the three types of dipolar couplings observed for the peptide group. For the general case, where the molecular alignment tensor lacks axial symmetry, there are eight solutions (related by mirror image symmetry about the xz , yz , and xy planes) which simultaneously satisfy all three dipolar couplings and have correct bond angles and lengths. For a dipeptide fragment, there are two additional unknowns: the backbone torsion angles ϕ and ψ and a total of six measured couplings. A grid search over ϕ and ψ , and calculation of the orientation of the dipeptide relative to the alignment tensor which yields the best fit (Powell minimization)¹⁶ between predicted and measured couplings for each ϕ/ψ point, is then used to search which ϕ/ψ combinations are most compatible with the measured couplings. Backbone ϕ and ψ torsion angles derived from such maps for the protein ubiquitin show excellent agreement with the crystal structure (Supporting Information).

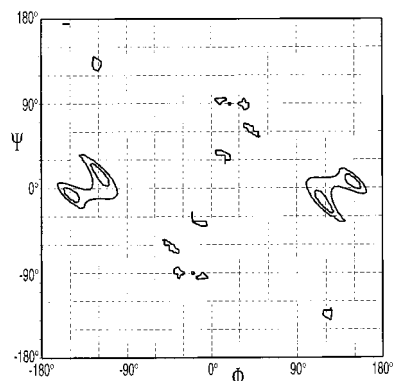


Figure 2. Contour map showing the value of the error function, $E = \frac{1}{6} [C_k(D^{\text{best fit}} - D^{\text{exp}})]^2$, as a function of the torsion angles ϕ and ψ of residue Thr²²⁴ in MAP30. The values of ϕ and ψ are systematically incremented in 5° steps. E is the minimum calculated using a program which searches for the dipeptide orientation in the alignment tensor frame which yields the best fit between measured and calculated data.¹⁶ The summation extends over the six couplings ($^1D_{\text{NH}}$, $^1D_{\text{CN}}$, and $^2D_{\text{CHN}}$) of the two peptide groups flanking Thr²²⁴, and the scaling factors C_k are 8.4 for $^1D_{\text{CN}}$, 3.0 for $^2D_{\text{CHN}}$, and 1 for $^1D_{\text{NH}}$.

The distribution of observed dipolar couplings for perdeuterated MAP30 in the liquid crystalline phase indicates an alignment tensor with $D_a = 17$, and a rhombicity R of 0.6.¹⁵ Figure 2 provides an example of a map, calculated in the above-described manner, which shows to what extent given pairs of ϕ and ψ angles of Thr²²⁴ are compatible with the measured dipolar couplings. As no dipolar coupling for a chiral center is included, the handedness of the polypeptide backbone cannot be determined from these data alone, but the region near $\phi/\psi = +120^\circ/0^\circ$ is strongly disallowed for steric reasons when using L-amino acids. Thus, for Thr²²⁴ in MAP30, at the end of its tenth β -strand, the dipolar coupling data indicate $\phi = -125 \pm 25^\circ$ and $\psi = 10 \pm 20^\circ$. If, for a given residue, multiple regions in the allowed area of ϕ/ψ space are compatible with the observed dipolar couplings, the correct region usually can be identified on the basis of ^1H and ^{13}C chemical shifts.¹⁷ Note that the C_2 -symmetric degeneracy of the contour map can be lifted when $^1D_{\text{C}\alpha\text{H}\alpha}$ is also included in the fitting procedure; however, this coupling may be more difficult to measure in large proteins.

It is anticipated that in perdeuterated proteins, where structure determination suffers from the lack of a large number of NOEs, addition of dipolar and torsion constraints will permit calculation of structures at a useful level of resolution. In this respect, it is important to note that in addition to improving convergence by constraining ϕ and ψ angles, the dipolar couplings also define the orientations of the dipeptide fragments relative to the alignment tensor.

The absence of large ^1H – ^1H dipolar interactions in a protein where all nonexchangeable hydrogens are deuterated permits the use of relatively strong alignment. Combined with the constructive use of relaxation interference, this makes it possible to measure accurately the inherently small one-bond $^{13}\text{C}'$ – ^{15}N and two-bond $^{13}\text{C}'$ – $^1\text{H}^{\text{N}}$ dipolar couplings, in addition to the one bond ^{15}N – $^1\text{H}^{\text{N}}$ dipolar coupling, even in large proteins and all from the same experiment. These values provide strong constraints when determining the protein structure.

Acknowledgment. We thank Frank Delaglio, Nico Tjandra, Marcel Ottiger, Rob Tycko, and Marius Clore for help and useful discussions.

Supporting Information Available: Contour plots analogous to Figure 2, showing the agreement between dipolar couplings and ϕ and ψ , for Q2–V5 in human ubiquitin; pulse sequence diagram and parameters used for measuring the spectra of Figure 1 (2 pages, print/PDF). See any current masthead page for ordering and Web access instructions. JA980862O

(14) Lipari, G.; Szabo, A. *J. Am. Chem. Soc.* **1982**, *104*, 4546–4558.

(15) Clore, G. M.; Gronenborn, A. M.; Bax, A. *J. Magn. Reson.* **1998**, *133*, 216–221.

(16) Tjandra, N.; Feller, S. E.; Pastor, R. W.; Bax, A. *J. Am. Chem. Soc.* **1995**, *117*, 12562–12566.

(17) Beger, R. D.; Bolton, P. H. *J. Biomol. NMR* **1997**, *10*, 129–142.